Scanning Microscopy

Volume 8 | Number 4 Article 23

12-28-1994

Bias Dependence of the Depletion Layer Width in Semi-Insulating GaAs by Charge Collection Scanning Microscopy

A. Castaldini
Universita' di Bologna

A. Cavallini
Universita' di Bologna, cavallini@bologna.infn.it

C. del Papa
Universita' di Bologna

M. Alietti
Facoltà di Ingegneria

C. Canali
Facoltà di Ingegneria

See next page for additional authors

Bias Dependence of the Depletion Layer Width in Semi-Insulating GaAs by Charge Collection Scanning Microscopy

Authors

A. Castaldini, A. Cavallini, C. del Papa, M. Alietti, C. Canali, F. Nava, and C. Lanzieri

Scanning Microscopy, Vol. 8, No. 4, 1994 (Pages 969-978) 0891-7035/94$5.00+.25
Scanning Microscopy International, Chicago (AMF O'Hare), IL 60666 USA

BIAS DEPENDENCE OF THE DEPLETION LAYER WIDTH IN SEMI-INSULATING GaAs BY CHARGE COLLECTION SCANNING MICROSCOPY

A. Castaldini[1], A. Cavallini[1,*], C. del Papa[1,2], M. Alietti[3], C. Canali[3], F. Nava[2,3] and C. Lanzieri[4]

[1]Dipartimento di Fisica, Universita' di Bologna, Via Irnerio 46, I-40126 Bologna, Italy; [2]INFN-Bologna, Via Irnerio 46, I-40126 Bologna, Italy; [3]Facoltà di Ingegneria, Via Campi, I-41100 Modena, Italy; [4]ALENIA S.p.A., Direzione Ricerche, Via Tiburtina, I-00131 Roma, Italy

(Received for publication July 20, 1994 and in revised form December 28, 1994)

Abstract

A procedure for the evaluation of the depletion region width of a Schottky barrier diode made on semi-insulating materials has been assessed and applied to gallium arsenide nuclear detectors. This procedure, which makes use of the optical beam induced current method of charge collection scanning microscopy, allows the direct measurement of the depletion layer width. By taking into account the high resistivity of the material under examination and measuring the diode reverse current, it is possible to evaluate the actual voltage applied at the depletion layer boundaries. It was found that, at low actual bias values, the voltage dependence of the depletion layer follows the usual square root power law, while at increasing voltages, it changes into a linear behavior. An explanation in terms of deep trap effect and trap field-enhanced capture cross-section is proposed even though further work must be done to explain the space charge width dependence on bias applied in terms of the deep trap influence.

Key Words: Charge collection microscopy, semi-insulating materials, depletion layer width, optical beam induced current, electron beam induced current, photocurrent profiles, conductivity, radiation detectors, detector active region, high resistivity materials.

*Address for correspondence:
Anna Cavallini
Dipartimento di Fisica,
Universita' di Bologna,
Via Irnerio 46,
I-40126 Bologna,
Italy

Telephone number: ++39 51 6305108
FAX number: ++39 51 6305153
Email: cavallini@bologna.infn.it

Introduction

Undoped semi-insulating (SI) gallium arsenide grown by liquid encapsulated Czochralski technique is currently attracting much interest because it is one of the most promising materials as a substrate for the fabrication of microwave integrated circuits. Furthermore, it has recently being used for developing detectors for a range of applications, including high energy physics as well as medical and molecular biology.

For the above reasons, extensive studies have been made on both structural and electrical characteristics of SI undoped GaAs with many investigation methods, such as photoetching Weyher *et al.* (1994), transmission electron microscopy Schloßmacher *et al.* (1992), and photo-induced current spectroscopy (Fang and Look, 1991).

Even though a few examples are reported in literature (Leamy, 1982, and references therein), charge collection scanning microscopy (CCSM) has not been applied to high resistivity materials so extensively as to semiconducting materials because it is widely thought, though seldom explicitly said, that charge collection scanning microscopy can be applied to "good" semiconductors only. However, it has been recently shown (Holt, 1994) that this assumption is wrong and that the beam induced current mode of CCSM can be usefully applied to semi-insulators as well as to wide-gap semiconductors.

In the literature, most of the investigations by electron beam induced charge collection microscopy which have been carried out on semi-insulating gallium arsenide are relevant to the microscopic characterization of the uniformity of undoped GaAs wafers (Tokumaru and Okada, 1984, 1985). In these investigations, the electron-beam-induced-current contrast in SI specimens is considered to arise mainly from recombination loss of induced current (Tokumaru and Okada, 1984).

The second statement usually implicit when speaking about Schottky barriers on insulators is that, contrary to the case of semiconductor specimens, the electric field is uniform over the whole sample length. The insulating samples would originally be near the state of depletion

as a whole, due to the built-in potential of the Schottky contact, leading to no modulation of the barrier depletion layer width W under an applied bias voltage.

This latter assumption sharply contrasts with experimental findings relative to Schottky devices working as radiation detectors (D'Auria and del Papa, 1992) from which it undoubtedly emerges that the detectors are not fully depleted. As a consequence, modeling of the electric field in SI gallium arsenide detectors is presently developing (McGregor *et al.*, 1992a, 1994; Chen *et al.*, 1994; Kubicki *et al.*, 1994) in order to explain the detector behaviour in terms of the actual space charge region width and charge carrier trapping effects.

This paper deals with charge collection scanning microscopy (CCSM) investigations on the depletion layer width (W) in SI gallium arsenide as a powerful tool for directly measuring the space charge region thickness. Electron beam induced current (EBIC) and optical beam induced current (OBIC) methods of CCSM have been applied in order to: **i**) achieve the image of the Schottky barrier depletion layer, and **ii**) measure its variations with the bias voltage applied. This analysis has uncovered a linear dependence of the depletion layer W on the voltage (V_a) given by the power supply and applied to the detector between ohmic and rectifying contacts. A study of the Schottky diode equivalent circuit has been performed to find the relationship between W and the effective voltage V_{eff} applied to the boundaries of the depletion layer. In this way, the usual quadratic trend of W as a function of the effective voltage applied has been found up to a value $V_{eff} = 50$ V, while for higher values the linear trend holds true. In order to verify the procedure adopted, a p^+-n junction on silicon has been tested in the same way as the GaAs diodes.

Materials and Methods

Two sets of specimens have been examined, the first one of semi-insulating (SI) ($\rho = 10^7$ Ω.cm) undoped gallium arsenide grown by the liquid encapsulated Czochralski (LEC) method and the second one of semiconducting floating zone silicon (phosphorus doped, majority carrier density N_D-$N_A = 10^{12}$ cm^{-3}). The semi-insulating GaAs samples [5 × 5 mm^2 in size and with thickness (t) ranging from 80 to 465 μm] have been prepared as follows: the Schottky barrier has been obtained by Au/Ti evaporation, and a Si-Pd solid phase epitaxy has been used as the ohmic contact (Nava, 1992). In the silicon samples, the p^+-n junction has been obtained by boron implantation, while the ohmic contact has been prepared by phosphorus implantation. A voltage source (Model 230, Keithley, Cleveland, Ohio) with very low (10^{-3} Ω) output impedance has been used to reverse bias the specimens in a range from 0 to

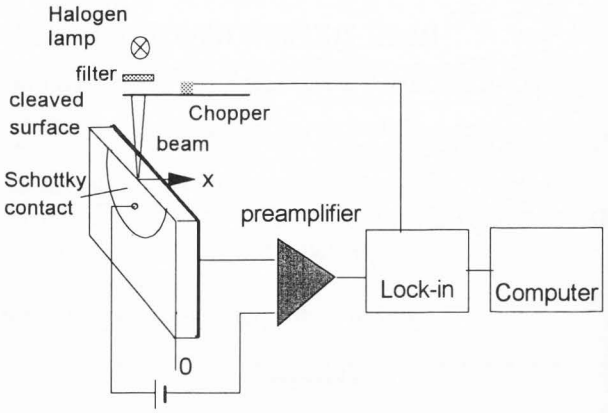

Figure 1. Principle of the electron/optical beam induced current detection method. The beam scans the sample cleaved surface in x-direction and the charge collection signal is amplified and then computer-stored.

120 V. The diode current-voltage characteristics have been analysed (Norde, 1979) and series resistance (R_S) and ideality factor (n) of the devices under test have been obtained. The beam induced current has been amplified by a feedback amplifier (Keithley 428). A lock-in amplifier has been used to minimize the noise penalty imposed by examining the diode depletion layer under as low as possible injection conditions.

The samples have been analyzed by charge collection scanning microscopy in "edge-on", also called "normal collector", configuration (Donolato, 1983) (Fig. 1). For this purpose, the cross-section view has been afforded by crystal cleavage and the cleaved edge of the device has been probed by the scanning beam.

The well known "barrier electron voltaic effect" at a junction (for a review, see Holt, 1989) has been used in order to evaluate the depletion layer width W and its changes with a resolution of a few micrometers. EBIC mode of scanning electron microscopy (SEM) utilizes the current due to the electron-hole pairs generated by the scanning electron beam which are separated by built-in field regions in the sample and finally collected by the rectifying junction. Similarly, OBIC mode of scanning optical microscopy (SOM) (Wilson and Sheppard, 1984; Castaldini and Cavallini, 1992) makes use of the pairs generated by a photon beam scanning the sample surface. The charge collection current (I_{cc}) modulates the microscopy cathode ray tube (CRT) intensity to obtain an image or it can be recorded as induced current profiles corresponding to the beam linescans on the sample surface.

In the OBIC analysis reported here, the probe light wavelength was 700 nm, the beam diameter at the sample surface was 2 μm and the photon flux 9.8 x 10^{15} photons.cm^{-2}.s^{-1}).

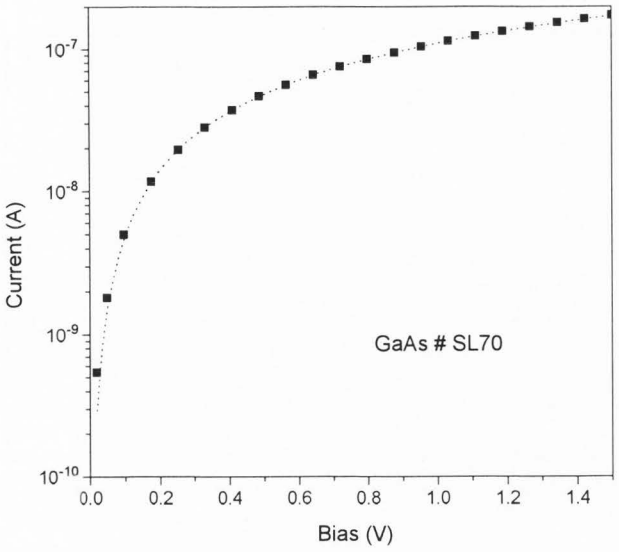

Figure 2. Forward current-voltage characteristic of a typical GaAs detector. The symbols ■ correspond to experimental data, the dashed line is their fit obtained by accounting for non-pure thermionic-emission current transport mechanism.

Results and Discussion

The current-voltage characteristic was obtained for each device. A typical example relevant to GaAs detectors is reported in Figure 2. Its shape indicates that the diode ideality factor and series resistance are high, suggesting that the pure thermionic emission over the barrier is not the only dominant mechanism and the contributions of other current-transport mechanisms must be taken into consideration (Sze, 1981; Donoval *et al.*, 1991). By accounting for these additional contributions (generation-recombination, leakage and tunneling currents), the semi-logarithmic plot of the current-bias voltage relationship has been fitted (dashed line in Fig. 2). From this line, we get that the ideality factor n is 1.16 and the series resistance R_S is 7.7×10^6 Ω. Although high if compared to values relevant to "good" metal-semiconductor barriers, the above values are very satisfying for a Schottky barrier on semi-insulating gallium arsenide (McGregor *et al.*, 1992b) and certainly good enough for adopting here the 'depletion' or 'abrupt' approximation about the metal-gallium arsenide barrier (Look, 1989).

In high resistance specimens, the carrier drift length (λ) is often small in comparison to the contact distance. When this happens, the locally induced polarization (Gunn, 1964) (in the present case, possibly due to the beam generated charges) can significantly reduce the barrier electron voltaic effects (Munakata, 1968, 1972; Holt, 1989). In the samples examined here, the barrier electron voltaic effects were meaningfully detectable in EBIC micrographs of gallium arsenide diodes (Fig. 3a), where the depletion layer W definitely appears as a bright area. However, in order to appreciate with the best accuracy the depletion layer width changes as a function of the reverse bias voltage, we preferred to quantitatively analyze OBIC profiles instead of EBIC ones. As a matter of fact, using a photon probe has allowed us to work in as low as possible injection conditions and then to avoid potentials locally induced by plasma effect (Alberigi Quaranta *et al.*, 1968) which could possibly modify the electric field under examination. Indeed, for GaAs, Leamy and Kimerling (1977) have demonstrated that high injection conditions may easily be obtained. Besides, it has been observed that surface charging easily occurs when an electron beam scans the detectors.

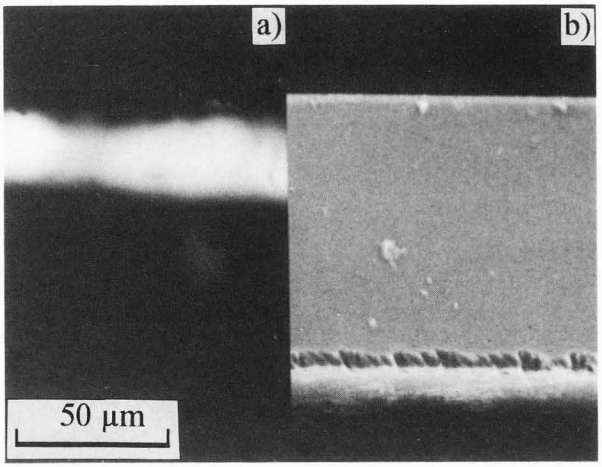

Figure 3. (**a**) EBIC micrograph of a GaAs detector diode (thickness t = 80 μm) showing the bright area which corresponds to the space charge region of unbiased diode; (**b**) secondary electron image of the same sample (Schottky barrier on the top side, beam energy E_b = 25 keV).

Figure 3a shows the EBIC micrograph of a GaAs detector diode from which it is seen that the depletion region does not fill the specimen up, while Figure 3b is the secondary electron image of the same detector, showing the Schottky contact on the top side and the ohmic contact on the bottom side. Clearly, care must be exercised when charge collection images, such as Figure 3a, taken for visual determination of the location and extension of the depletion region, are to be properly interpreted (Leamy, 1982). Current amplifier black level and gain are purposefully adjusted to improve the cosmetic quality of EBIC images, but this method can lead to serious errors of interpretation of the relative video

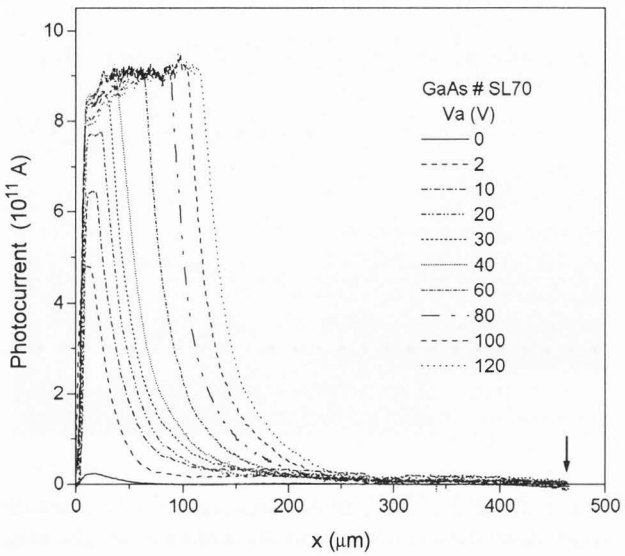

Figure 4. OBIC profiles obtained by scanning a reversely biased GaAs diode (465 μm thick) across the Schottky barrier (the power supply voltages V_a are reported in the legend).

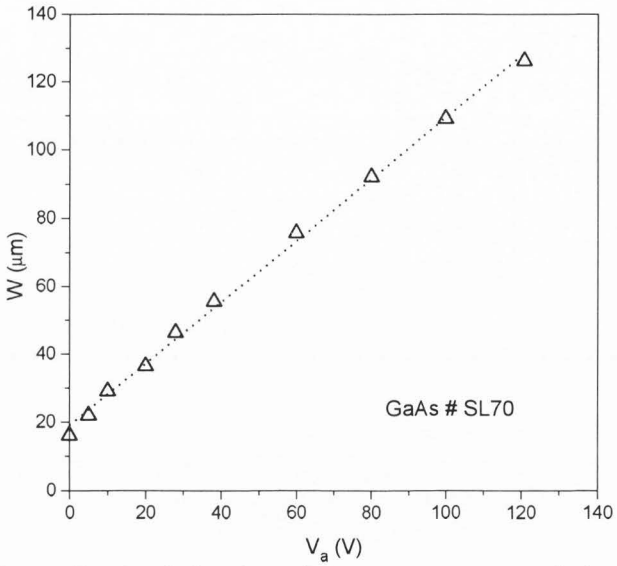

Figure 5. Depletion layer W versus reverse applied voltage V_a (given by the power supply) for the same GaAs detector as Figure 4 (the dotted line corresponds to the fitting expression).

signal strength. In the present case, the microscope parameters have been adjusted to evidence the depletion layer extent, consequently loosing any details on its bounds which actually are less sharp than in the present micrograph.

Optical beam induced current profiles, corresponding to different reverse bias voltages V_a, given by the power supply between ohmic and rectifying contacts, are shown in Figure 4. They have been obtained by beam linescans across the Schottky barrier edge-on (x-axis), with the Schottky contact surface normal to the paper plane and coinciding with the y-axis. It is worth noting that the current profiles do not exhibit their maximum value at exactly x = 0, as should be expected, but present a current rise up to a beam coordinate equal to a few micrometers. This is due to the following reasons:

(1) the scanning beam size is 2 μm; therefore, the beam spot (and as a consequence, the generation volume) does not wholly enter the sample when the beam translator is just (or just behind) at the coordinate x = 0 (which corresponds to the sample edge), but from this position, without interruption, it enters the diode; and

(2) the surface debris, due to treatments performed for reducing the detector leakage current, reasonably induces "surface" states which significantly increase the local charge carrier recombination in the layer just below the Schottky barrier; this is imaged as a dark region in the EBIC micrograph (Fig. 3a) as well.

About the peak shape of the current profiles at low voltages, it is worth noting that the photon flux is low (9.8×10^{15} photons.cm^{-2}.s^{-1}) and the generated carrier density is comparable to the trap concentration (as well known, in LEC GaAs, the major trap EL2 concentration is of the order 10^{16} cm^{-3}). Consequently, carrier trapping at deep levels partially occurs up to the electric field (E) is high enough that the collection efficiency equals to 100%. This occurs at $V_a \cong 30$ V (Fig. 4) for GaAs diodes, corresponding to $E \approx 4\text{-}5 \times 10^3$ V/cm, and $V_a \cong 2$V (as will be shown in Fig. 6) for Si diodes, corresponding to $E \approx 8 \times 10^2$ V/cm. This difference can be understood taking into account that GaAs is undoped, compensated material ($\rho = 10^7$ Ω.cm) with a large trap concentration, while silicon is semiconducting material ($\rho = 3000$ Ω.cm).

The depletion layer width W, identified with the photocurrent profile half maximum width, results in a linear function of the reverse bias V_a (Fig. 5):

$$W = 19.0 + (0.9 \times V_a) \qquad (1)$$

where W is expressed in μm when V_a is given in volts.

This finding came out to be reproducible with high accuracy and with a regression coefficient R $\geq$ .999 in all experiments. The systematic error due to the above points (i) and (ii) produces a shift of the depletion layer curve but does not change its behaviour since the current profiles exactly overlap in the x-range of current rise.

In order to check the procedure adopted for the determination of W, silicon p^+-n detectors have been also examined. Figure 6 shows OBIC profiles relevant to linescans of a reverse-biased p^+-n junction in the same configuration as in Figure 1. In this case, too, a current

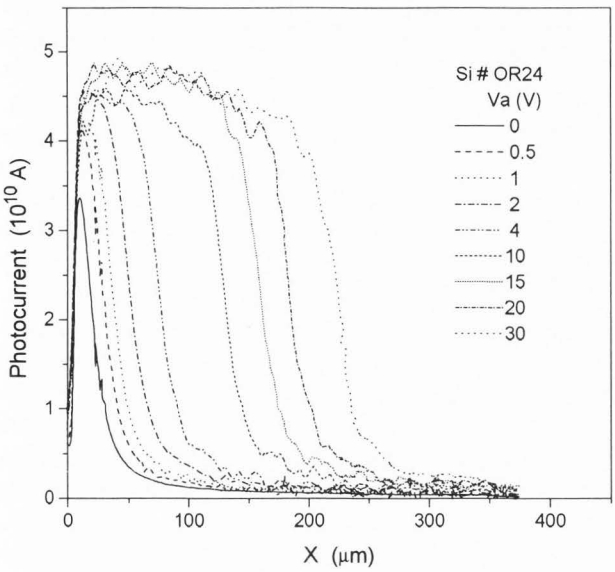

Figure 6. OBIC profiles across the reversely biased depletion region of a silicon p^+-n detector. The applied V_a are reported in the legend.

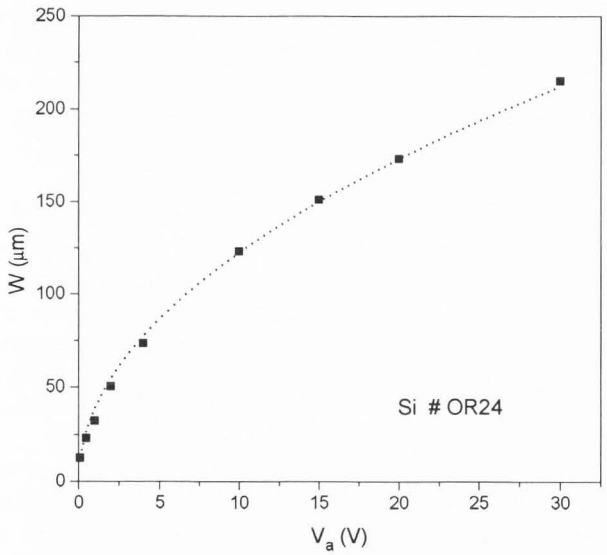

Figure 7. Depletion layer width W as a function of the reverse bias V_a in the same Si p^+-n detector as Figure 6. The symbols ■ refer to the experimentally determined width values, the dotted diagram has been obtained by fitting the data using equation (2) with $N_D - N_A = 9 \times 10^{11}$ cm^{-3}.

---

rise equal to that relevant to GaAs detectors occurs for the same reasons given above. Contrary to that stated above about the GaAs detectors, the well known square root power relationship between W and V_a has been obtained from the junction depletion layer width W measured by the photocurrent profiles (Fig. 7). Fitting the experimental data to the usual expression (Sze, 1981)

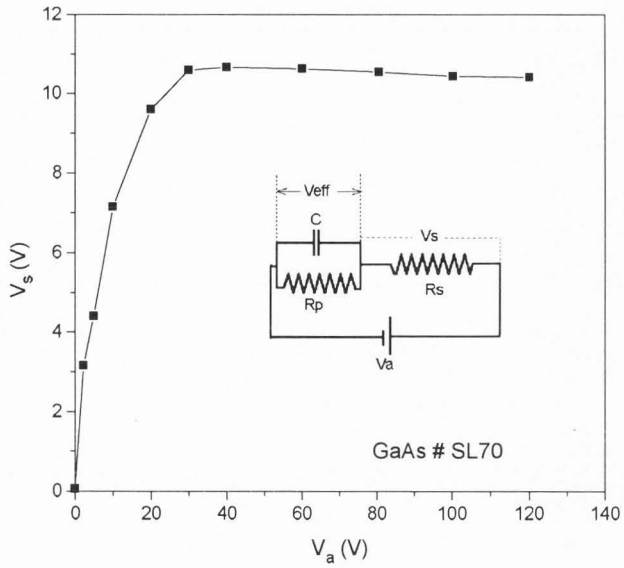

Figure 8. Voltage V_S at the undepleted region boundaries versus reverse bias V_a applied to the detector. The inset shows the diode equivalent circuit with C and R_P capacitance and parallel resistance, respectively, of the depletion layer W and R_S series resistance of the bulk material, and the relevant voltage drops V_{eff} and V_S.

$$W = [\{2\epsilon\epsilon_0 / \{q\,(N_D - N_A)\}\}\,(V_{bi} - V_a - kT)]^{1/2} \quad (2)$$

where ϵ is the silicon dielectric constant, ϵ_0 the vacuum permittivity, V_{bi} the built-in junction potential, k the Boltzmann constant, T the temperature and q the elementary charge, enabled the best-fit value of the parameter $(N_D\text{-}N_A)$ to be found. This value, equal to 9×10^{11} cm^{-3}, coincides within the experimental uncertainty with the majority carrier concentration due to the specimen doping level. All the above reported experiments have been carried out at room temperature (294K).

By comparing GaAs and Si results reported in Figures 5 and 7, respectively, we can observe that while the silicon depletion layer exhibits the well known root square dependence on the applied voltage V_a, the GaAs samples show a linear dependence.

In order to explain this apparently anomalous behavior of GaAs diodes, the detector equivalent circuit has been analyzed by taking into account the high resistivity of GaAs bulk material ($\rho = 10^7$ Ω.cm) and measuring the diode reverse current (i_l) against the applied voltage (V_a). This analysis has clearly pointed out that a non-negligible voltage drop (V_S) occurs across the undepleted region of the GaAs detector. The inset of Figure 8 shows the detector equivalent circuit where C and R_P are the capacitance and the parallel resistance of the space charge layer W, while R_S is the series resistance of the undepleted bulk layer. The voltage drop (V_S) across the undepleted bulk layer has been calculated by

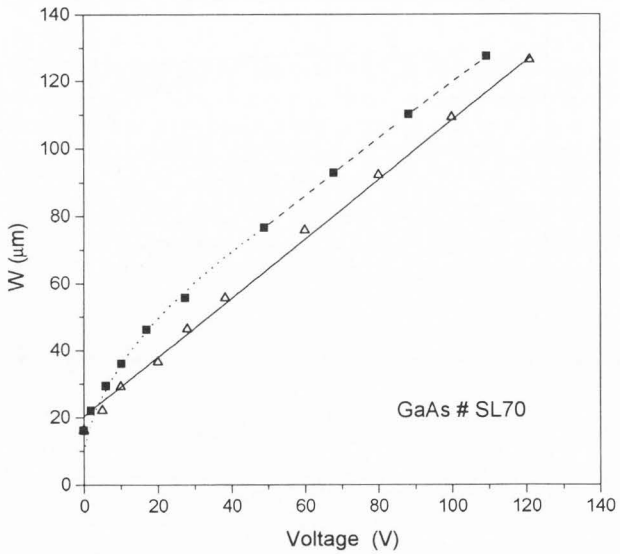

Figure 9. Depletion layer width W versus bias voltage. The symbols Δ are values of W plotted against the applied voltage V_a given by the power supply, while the symbols ■ are values of W plotted against the effective voltage drop V_{eff} at the space charge region boundaries.

---

the expression:

$$V_S = \rho\ [\{t - W(V_a)\} / S]\ i_l\ (V_a) \qquad (3)$$

where t, sample thickness, corresponds to the distance between Schottky and ohmic contacts, S is the diode area, and i_l and W have been defined above.

V_S is reported in Figure 8 as a function of the applied voltage V_a. As can be seen, V_S increases with increasing V_a up to a saturation value equal to about 11 V. Correspondingly, the effective voltage (V_{eff}) actually applied between the boundaries of the depletion layer becomes $V_{eff} = V_a - V_S$. By taking equation (1) into account again, the evaluation of the effective voltage V_{eff} allows to correct the voltage dependence of the depletion layer in GaAs detectors.

The resulting values are reported in Figure 9, where the symbols Δ refer to values of W relative to the voltage V_a applied to the specimen, while the symbols ■ refer to values of W relative to the effective voltage drop, V_{eff}, applied between the depletion region boundaries. As can be observed from the data of Figure 9, at low effective voltages ($V_{eff} < 50$ V) W increases roughly with the square root of V_{eff} and with a corresponding density of ionized donors $N_d = 1.26 \times 10^{13}$ cm^{-3}, while for $V_{eff} > 50$ V, W increases almost linearly with the reverse bias voltage. This latter linear dependence of W on V_a has been already observed (D'Auria and del Papa, 1992) and calculated (Kubicki *et al.*, 1994) for high applied voltages, $V_a \geq 100$ V. Recently, using alpha particle irradiation data, McGregor *et al.* (1994) found that "a nearly linear relationship between detector voltage and active region depth" exists. To explain such an effect, ionized deep traps and their influence on the electric field distribution must be accounted for. McGregor's model including field enhanced capture cross-section of EL2 can be invoked. It proposes that at low fields, the electron capture rate is low due to a small capture cross-section of the EL2 defect, and that the ionized EL2 concentration is well approximated by the Fermi statistics referring to the quasi-Fermi level. When higher voltages are applied, so that an electric field $\geq 10^4$ V/cm results, the electron capture cross-section of the EL2 trap dramatically increases (Kaminska *et al.*, 1982; Prinz and Rechkunov, 1983; Johnson *et al.*, 1987, 1990; Ralph and Grischkowsky, 1991). The electron emission rate becomes, therefore, the limiting process of the EL2 centers filling and, as a consequence, a quasineutral region results at high bias voltages. This model well matches our results: at low bias voltages the behaviour of the depletion layer width is controlled by the free carrier concentration and the active region width increases proportionally to $\sqrt{V}$. When the bias voltage V_{eff} approaches a value corresponding to an electric field near to $\approx 10^4$ V/cm (50 V in the example reported in Fig. 9), a linear dependence results as a consequence of the quasineutral region generation.

Conclusions

Electrical beam induced current and optical beam induced current methods have been applied in order to investigate the thickness (W) of the space charge layer in semi-insulating GaAs diodes as well as to accurately measure its changes with the reverse bias voltage applied to the detectors and with the effective voltage applied between the boundaries of the space charge layer.

The OBIC procedure adopted to directly measure W has also been tested on silicon diodes in order to analyze the behavior of a p^+-n junction depletion layer as a function of the bias voltage. The well known root square dependence of W on V_a has been found, which demonstrates the procedure reliability.

The results referring to GaAs diodes have demonstrated that the depletion layer thickness evaluation can be misleading if the detector's high resistivity is not taken into the due consideration, since the actual voltage drop between the depletion layer boundaries can significantly differ from the voltage applied to the detector.

The accurate measurement of the depletion layer width is of fundamental importance to evaluate detector performance. More theoretical and experimental work has to be done in order to explain both the root square and the linear dependencies of space charge width on the effective voltage.

References

Alberigi Quaranta A, Taroni A, Zanarini G (1968) Plasma time in semiconductor detectors. IEEE Trans. Nucl. Sci. **15**: 373-380.

Castaldini A, Cavallini A (1992) Recombination activity of individual extended defects in silicon. In: Defect Engineering in Semiconductor Growth, Processing and Device Technology. Ashok S, Chevallier J, Sumino K, Weber E (eds.). Materials Research Society, Pittsburgh. **262**, 223-233.

Chen JW, Ebling D, Eiche C, Fiederle M, Frömmichen T, Hug P, Irsigler R, Jantz W, Ludwig J, Plötze T, Rogalla M, Runge K, Stibal R (1994) Characterization of semi-insulating GaAs for detector fabrication. In: European Gallium Arsenide and Related III-V Compounds Applications Symposium. Naldi CU (ed.). IEEE Microwave Theory and Techniques Society Publisher, Torino (Italy). pp. 139-142.

D'Auria S, del Papa C (1992) Charge collection and electric field in gaas particle detectors. In: GaAs Detectors and Electronics for High Energy Physics. del Papa C, Pelfer PG, Smith K (eds.). World Scientific, Singapore. pp. 246-254.

Donolato C (1983) Evaluation of diffusion lengths and surface recombination velocities from electron beam induced current scans. Appl. Phys. Lett. **43**: 120-122.

Donoval D, Barus M, Zdimal M (1991) Analysis of I-V measurements on PtSi-Si Schottky structures in a wide temperature range. Solid-St. Electron. **34**: 1365-1373.

Fang ZQ, Look DC (1991) Comparison of deep centers in semi-insulating liquid-encapsulated Czochralski and vertical-gradient freeze GaAs. J. Appl. Phys. **69**: 8177-8183.

Gunn JB (1964) A general expression for electrostatic induction and its application to semiconductor devices. Solid-St. Electron. **7**: 739-742.

Holt DB (1989) SEM microcharacterization of semiconductors. Holt DB, Joy DC (eds.). Academic Press, London. pp. 241-338.

Holt DB (1994) Local grain boundary property measurements. In: Polycrystalline Semiconductors III - Physics and Technology. Strunk HP, Werner JH, Fortin B, Bonnaud O (eds.). Solid State Phenomena **37-38**. Trans. Tech. Publ., Zürich. pp. 171-182.

Johnson DA, Myhajlenko S, Edwards JL, Maracas GN, Roedel RJ (1987) Imaging of deep level domains in semi-insulating GaAs by voltage contrast. J. Appl. Phys. **51**: 1152-1154.

Johnson DA, Myhajlenko S, Edwards JL, Maracas GN, Roedel RJ (1990) Thermal and spectral dependence of low-frequency oscillations in semi-insulating GaAs:In. J. Appl. Phys. **67**: 300-306.

Kaminska M, Parsey JM, Lagowski J, Gatos HC (1982) Current oscillations in semi-insulating GaAs associated with field-enhanced capture of electrons by the major deep donor EL2. Appl. Phys. Lett. **41**: 989-991.

Kubicki T, Lübelsmeyer K, Ortmanns J, Pandoulas D, Syben O, Toporowsky M, Xiao WJ (1994) Calculation of the electric field in GaAs particle detectors. Nucl. Instrum. Meth. Phys. Res. A **345**: 468-472.

Leamy HJ (1982) Charge collection scanning electron microscopy. J. Appl. Phys. **53**: R51-R80.

Leamy HJ, Kimerling LC (1977) Electron beam induced annealing of defects in GaAs. J. Appl. Phys. **48**: 2795-2803.

Look DC (1989) Electrical Characterization of GaAs Materials and Devices. Wiley, New York. pp. 45-48, 151-158.

McGregor DS, Knoll GF, Eisen Y, Brake R (1992a) Fabrication and evaluation of room temperature operated radiation detectors processed from undoped LEC bulk gallium arsenide material. Nucl. Instrum. Meth. Phys. Res. A **322**: 487-492.

McGregor DS, Knoll GF, Eisen Y, Brake R (1992b) Development of bulk GaAs room temperature radiation detectors. IEEE Trans. Nucl. Sci. **5**: 1226-1236.

McGregor DS, Rojeski RA, Knoll GF, Terry FL Jr, East J, Eisen Y (1994) Evidence for field enhanced electron capture by EL2 centers in semi-insulating GaAs and the effect on GaAs radiation detectors. J. Appl. Phys. **75**: 7910-7915.

Munakata C (1968) Voltage signal due to electrical-beam-induced-conductivity in semiconductors. Jpn. J. Appl. Phys. **7**: 1051-1055.

Munakata C (1972) Improvement of the β-conductivity method of measuring electric field intensity in semiconductors by a pulsed electron beam. J. Phys. D: Appl. Phys. **5**: 1000-1004.

Nava F (1992) GaAs detector fabrication in Modena. In: GaAs Detectors and Electronics for High Energy Physics. del Papa C, Pelfer PG, Smith K (eds.). World Scientific, Singapore. pp. 121-129.

Norde H (1979) A modified forward I-V plot for Schottky diodes with high series resistance. J. Appl. Phys. **50**: 5052-5055.

Prinz VYa, Rechunov SN (1983) Influence of a strong electric field on the carrier capture by non-radiative deep-level centers in GaAs. phys. stat. sol. (b) **118**: 159-166.

Ralph SE, Grischkowsky (1991) Trap-enhanced electric fields in semi-insulators: The role of electrical and optical carrier injection. Appl. Phys. Lett. **59**: 1972-1974.

Schloßmacher P, Rüfer H, Urban K (1992) TEM investigations of defects in undoped semi-insulating

GaAs crystals. In: Microscopy of Semiconducting Materials 1991. Inst. Phys. Conf. Ser. **117**. Cullis AG, Long NJ (eds.). Institute of Physics, Bristol. pp. 337-342.

Sze SM (1981) Physics of Semiconductor Devices. Wiley, New York (2nd ed.). pp. 245-249, 259-306.

Tokumaru Y, Okada Y (1984) Electron-beam-induced charge collection microscopy of undoped LEC GaAs. Jpn. J. Appl. Phys. **23**: L64-L66.

Tokumaru Y, Okada Y (1985) SEM-EBIC investigations of semi-insulating undoped LEC-GaAs. Jpn. J. Appl. Phys. **24**: L364-L366.

Weyher JL, Sonnenberg K, Schober T (1994) A new approach for studying individual microdefects in SI GaAs by a combined use of IR microscopy, photoetching and TEM. In: 8th Conference on Semi-Insulating III-V Materials. Godlewski M (ed.). Inst. Phys., Polish Acad. of Sci. Publisher, Warsaw. 105-110.

Wilson T, Sheppard C (1984) Scanning Optical Microscopy. Academic Press, London. pp. 45-65.

Discussion with Reviewers

A. Jakubowicz: In Figure 4, one can see that not only the width at half-maximum increases with voltage, but also the intensity measured at maximum. At low voltages, there is a clear increase of the intensity with voltage: above 30 V, the maximum intensity saturates. This intensity versus voltage dependence is very similar to the curve in Figure 8. In both cases, the curves saturate at about 30 V. Can this similarity be explained? Is it accidental?

Authors: This similarity is accidental: in the detector we referred to in Figures 4 and 8, this coincidence occurs, while in other detectors investigated it does not occur.

A. Jakubowicz: At 0 V and at low bias voltages (up to about 30 V), the curves in Figure 4 have a peak shape (there is no plateau up to about 30 V, which means that at each beam position different number of carriers are collected). The authors use the width at half-maximum as a measure of the depletion layer width, which, at low and medium voltages, is strongly affected by the decaying part of the curves. Can the authors, in a general case, distinguish between two possible contributions to the width at half-maximum: (i) processes in the electric field of the depletion layer, and (ii) diffusion in the neutral material?

M. Kittler: You are identifying the depletion layer width by the half-height width of the photocurrent profile. This would be absolutely true if there would be a constant charge-collection within the depletion layer but a zero charge-collection (or at least a very small collection) in the neutral semiconductor material outside the depletion region. Analyzing the experimental OBIC profiles, it seems to me that especially the profiles taken for SI GaAs (Fig. 4) exhibit a clear diffusion controlled decay {photocurrent $\propto \exp(-x/L)$} whereas the profiles taken for Si (Fig. 6) look to be less influenced by the diffusion current coming from the neutral region. This might be one reason for the fact that the (half)width-versus-voltage dependency is harder to interpret for SI GaAs. Please comment.

Furthermore, to identify the transition from drift to the diffusion controlled photocurrent in the experimental profile I(x), Oelgart *et al.* (1981) plotted dI(x)/dx versus the probe position x and suggested that the minimum of this plot describes the border of the depletion region. Using this procedure for the determination of the width-versus-voltage dependency, they were even able to distinguish between different types of dopant profiles (abrupt, linearly graded, etc.). Could this method of identifying the depletion layer width also be useful in your case, especially for the SI GaAs material?

Authors: The most reliable method to distinguish between the drift-controlled region (that is the depletion layer) and the diffusion-controlled region undeniably consists in the determination of the minimum value of the derivative of the photoinduced current profile I versus probe position x, as reported in Oelgart *et al.* (1981). In the present case, however, we could not apply this method owing to the reasons below.

Due to the low voltages applied and the high resistivity of the semiconducting silicon diodes investigated, the depletion layer electric field was expected to be very low. To avoid any electric field perturbation, the scanning beam light intensity (and thus, the generation rate) was reduced as low as possible. The noise penalty imposed by examining the device cleaved edge in such conditions caused a wide dispersion in the data relevant to the minimum of the derivative dI(x)/dx. Therefore, the procedure based on the plot of dI(x)/dx did not yield the most appropriate result when applied to devices realized with such high resistivity silicon.

Since the photocurrent profiles were approximately square-shaped for $V_a \geq 2V$ (thus, only slightly influenced by the carrier diffusion), we adopted the photocurrent profile half-height width as measurement of the depletion layer width.

For consistency in the analysis of all diodes, we applied the same method to the semi-insulating GaAs Schottky diodes, too. Nevertheless, we analyzed the photocurrent profiles taken for GaAs also with the "derivative minimum procedure". We obtained the same bias dependence of the depletion layer (square root at low voltages and linear at higher voltages), while the numerical values were little higher ($\approx 5\%$).

With respect to the uniform SI GaAs material here

investigated, we analyzed only Schottky barrier diodes, where there was no problem of dopant profile determination. However, Oelgart's procedure should expectedly work when applied to diffused p-n junctions.

D.B. Holt: The use of charge collection scanning light microscopy to measure the depletion layer width and the demonstration of the importance of allowing for the significant drop of potential across the large series resistance in these samples is very satisfying. The micrographs in Figure 3, however, suggests a number of questions. Figure 3a shows significant variations in both the width and brightness of the depletion layer. This would appear to correspond to differences in the height and the position of the right-hand edge of line scan peaks like those in Figure 4. These in turn correspond to variations in W and in the field or collection efficiency of the material in the depletion region from point to point over the Schottky contact. How large, quantitatively, are these variations? Are they large enough to correspond to significant changes in the value of doping density? Are they large enough to affect detector device performance?
Authors: OBIC investigations have been performed on several beam scan lines for each device examined just because of the reason reported by the Reviewer. We measured variations within the range 5-10% in the depletion layer value, without any effect on its voltage dependence. The observed variations surely affect the detector device performance since they correspond to significant inhomogeneities in the trapping center density (the material is no intentionally doped).

D.B. Holt: In Figure 3a, the **top** edge of the depletion region image shows large variations. This corresponds apparently to changes in the position (depth) of the metal/GaAs interface, due perhaps to uneven penetration or diffusion. Is this the case or is some other effect such as masking of the beam by surface debris responsible?
Reviewer IV: Why are the OBIC-current (observable in Figs. 4 and 6) and the EBIC-current (observable in Fig. 3a) so low at the metal-semiconductor-interface of the Schottky diodes? Usually, the electric fields inside a Schottky diode are highest at the interface between the metallization and the semiconductor. Thus, a complete separation of the electron hole pairs and, thus, the highest current is expected at this interface.
Authors: To evidence the depletion layer the amplifier black level and gain have been adjusted to enhance the depletion layer brightness. Owing to this adjustment, the actual depletion layer width seems, in the EBIC micrograph, narrower than it actually is and results from the beam line scan profiles. However, a "surface" recombination region exists, which is due to presence of trapping centers due to surface debris. It can be, conversely, excluded uneven penetration or diffusion since the Schottky barrier is evaporated and no successive thermal treatments are performed.

J.C.H. Phang: A beam chopper and a lock-in amplifier are used in the experiment. What is the beam chopping frequency and is there likely to be effects of the C, R_P and R_S combination?
Reviewer IV: What is the value of the used chopping frequency? This is important for investigations if deep traps are periodically recharged in the specimen.
Authors: We used two beam chopping frequencies: 16 and 72 Hz. With so low values, the output signal was unaffected by our detector characteristic R_PC factor. Considering results from the I-V curve reported in Figure 2 as an example, the relevant values of R_S, R_P and C are $7.7 \times 10^6\ \Omega$, $4.5 \times 10^6\ \Omega$, and 2.2 pF, respectively, at $V_a = 40$ V that corresponds to a depletion layer W equal to 70 μm (diode diameter = 2 mm). In all the tested detectors, the diode constant R_PC was of the order 10^{-5} s, which is negligible in comparison to the light probe period.

J.C.H. Phang: It is necessary to use a beam chopper-lock-in amplifier for this experiment instead of direct OBIC measurements?
Authors: In principle, it is possible to perform direct OBIC measurements, too. Indeed, preliminary direct measurements have been performed to check possible frequency effects. These measurements gave the same results as those obtained by chopped light induced currents, measured with a lock-in amplifier. However, as the former data were more noisy, since the photon flux is so low that the photo-generated carrier density is comparable to the trap concentration, we preferred to work with photocurrent profiles obtained by the lock-in technique.

Reviewer IV: Why is the boundary of the depletion layer inside the specimen sharp? If the net charge carrier density on the GaAs substrate would be really very low (as could be expected by a resistivity of $\rho = 10^7$ Ω.cm) this sharp border could not be explained. What about the role of deep centers?

What is the physical reason for a depletion layer width of only $W = 19$ μm for an unbiased Schottky diode? Using your equation (2), a net doping of $N_D = 3.3 \times 10^{12}$ cm^{-3} can be calculated! So, the GaAs was not semi-insulating? What about the influence of deep centers (point defects)?
Z.Q. Fang: According to the R_S model, an effective voltage V_{eff} of $\sim$ 50 V with a density of ionized donors $N_D = 1.26 \times 10^{13}$ cm^{-3} is roughly deduced from the

corrected curve of W versus V_{eff} in Figure 9. However, the N_D seems too small and cannot be EL2, which need to be explained. Also, the linking of data points (■) seems to be with some uncertainty. Please comment.

Authors: The sharpness of the depletion layer edge inside the sample can be explained by the following two causes.

(1) As with the depletion layer edge near the Schottky barrier (see the relevant answer to Dr. Holt), we adjusted the microscope working conditions to enhance the depletion layer brightness. Owing to this adjustment, in the EBIC micrograph the boundary of the depletion layer inside the specimen is sharper and, consequently, the depletion layer width narrower than it actually is from the current profiles (Fig. 4).

(2) As suggested by both these Reviewers, the deep-level center role, too, need to be considered. This clearly arises from Figure 9, where the density of free carriers $N_D = 1.26 \times 10^{13}$ cm^{-3} (found by fitting all the experimental data of W up to 50 V and not from a single value of W) is too small to be accounted for EL2 and too large to be accounted for the net doping density. It should be noted that for samples with deep-level trap concentrations comparable to or larger than the doping concentration, the free carrier density in the depletion width expression is equal to the difference between the doping density (N_D - N_A) plus the ionized donor-type deep level density and the sum of all deep levels below the Fermi level. Similar considerations are reported by Lai *et al.* (1993). It is worth noting that in our GaAs detectors, several deep levels have been found (Castaldini *et al.*, 1995), both donor-type and acceptor-type, and that the fitting value we are speaking about refers to a W range, where different bias conditions (and, consequently, Fermi level position and deep level occupancy) have been used. Thus, the fitting value N_D is meaningful only if explained as free carrier density in the depletion width due to interaction between shallow and deep donor levels and "averaged" over the whole range of bias where the fitting procedure has been performed.

About the linking of data points, we used two different linking curves (dotted and dashed) to put into evidence the two voltage dependencies of W. Some uncertainty in the data linking occurs in this interval, since the transition from the square root dependency to the linear dependency cannot be sharp due to its dependency on the EL2 capture cross section change.

Reviewer IV: Only two GaAs specimens, with thicknesses 80 μm and 465 μm, have been investigated. So, why have you not investigated specimens in the thickness range 80 to 465 μm?

Z. Fang: To confirm the series resistance (R_S) model, presented in this paper, it is better to provide a comparative result on two SI GaAs samples with different thickness to show the effect of R_S.

Authors: We investigated several samples with different thickness. However, in this paper, we focused our attention on specimens about 100 μm and 400-500 μm thick because these two values are, or have been, the most technologically interesting ones for the application as radiation hard detectors. Indeed, the 100 μm thick detectors recently demonstrated to be the most efficient ones, while the 400-500 μm thick ones have being used up to now. Diagrams and micrographs reported in the text refer to "typical examples" of a general behavior.

M. Kittler: How strong could a misorientation (i.e., border of depletion layer inclined to the beam direction) affect the accuracy of determination of the depletion layer width?

Authors: The determination of the depletion layer width (W) was made in edge-view configuration with the junction surface parallel to the light beam so as the cleaved surface was inclined in respect to the scanning probe. The cleaved surface-microscope distance was kept constant to work with in-focus conditions. In this way, the misorientation problem was minimized, which otherwise would have been considered. Indeed, the misorientation would affect the accuracy of the determination of the depletion layer width depending on the angle between cleavage plane and junction plane (in the present case, the plane {100}).

Additional References

Castaldini A, Cavallini A, del Papa C, Fuochi G, Alietti M, Canali C, Nava F, Paccagnella A, Lanzieri C (1995) Defects induced by protons and γ-rays in semi-insulating GaAs detectors. In: Microstructure of Irradiated Materials. Robertson IM, Zinkle SJ, Rehn LE, Phytian WJ (eds.). Materials Research Society, Pittsburgh. **374**, 523-528.

Lai ST, Nener BD, Faraone L, Nassibian AG (1993) Characterization of deep-level defects in GaAs irradiated by 1 MeV electrons. J. Appl. Phys. **73**: 640-647.

Oelgart G, Fiddicke J, Reulke R (1981) Investigation of minority-carrier diffusion lengths by means of the scanning electron microprobe (SEM). phys.stat.sol. (a) **66**: 283-292.